# AFM Review Study on Pox Viruses and Living Cells

F. M. Ohnesorge,* J. K. H. Hörber,* W. Häberle,* C.-P. Czerny,# D. P. E. Smith* and G. Binnig*
IBM Research Division, *Physikgruppe München, D-80799 München, Germany, and #Veterinary Institute of the University of Munich, D-80799 Munich, Germany

ABSTRACT Single living cells were studied in growth medium by atomic force microscopy at a high—down to one image frame per second—imaging rate over time periods of many hours, stably producing hundreds of consecutive scans with a lateral resolution of ~30–40 nm. The cell was held by a micropipette mounted onto the scanner-piezo as shown in Häberle, W., J. K. H. Hörber, and G. Binnig. 1991. Force microscopy on living cells. *J. Vac. Sci. Technol.* B9:1210–0000. To initiate specific processes on the cell surface the cells had been infected with pox viruses as reported earlier and, most likely, the liberation of a progeny virion by the still-living cell was observed, hence confirming and supporting earlier results (Häberle, W., J. K. H. Hörber, F. Ohnesorge, D. P. E. Smith, and G. Binnig. 1992. In situ investigations of single living cells infected by viruses. *Ultramicroscopy.* 42–44:1161–0000; Hörber, J. K. H., W. Häberle, F. Ohnesorge, G. Binnig, H. G. Liebich, C. P. Czerny, H. Mahnel, and A. Mayr. 1992. Investigation of living cells in the nanometer regime with the atomic force microscope. *Scanning Microscopy.* 6:919–930). Furthermore, the pox viruses used were characterized separately by AFM in an aqueous environment down to the molecular level. Quasi-ordered structural details were resolved on a scale of a few nm where, however, image distortions and artifacts due to multiple tip effects are probably involved—just as in very high resolution (<15–20 nm) images on the cells. Although in a very preliminary manner, initial studies on the mechanical resonance properties of a single living (noninfected) cell, held by the micropipette, have been performed. In particular, frequency response spectra were recorded that indicate elastic properties and enough stiffness of these cells to make the demonstrated rapid scanning of the imaging tip plausible. Measurements of this kind, especially if they can be proven to be cell-type specific, may perhaps have a large potential for biomedical applications. Images of these living cells were also recorded in the widely known (e.g., Radmacher, M., R. W. Tillmann, and H. E. Gaub. 1993. Imaging viscoelasticity by force modulation with the atomic force microscope. *Biophys. J.* 64:735–742) force modulation mode, yet at one low modulation frequency of ~2 kHz. (Note: After the cells were attached to the pipette by suction, they first deformed significantly and then reassumed their original spherical shape, which they also acquire when freely suspended in solution, to a great extent with the exception of the portion adjusting to the pipette edge geometry after ~0.5–1 h, which occurred in almost the same manner with uninfected cells, and those that had been infected several hours earlier. This seems to be a process which is at least actively supported by the cellular cytoskeleton, rather than a mere osmotic pressure effect induced by electrolyte transport through the membrane. Furthermore, several hours postinfection (p.i.) infected cells developed many optically visible refraction effects, which appeared as small dark spots in the light microscope, that we believed to be the regions in the cell plasma where viruses are assembled; this is known from the literature on electron microscopy on pox-infected cells and referred to there as "virus factories" (e.g., Moss, B. 1986. Replication of pox viruses. *In* Fundamental Virology, B. N. Fields and D. M. Knape, editors. Raven Press, New York. 637–655). Therefore, we assume that the cells stay alive during imaging, in our experience for ~30–45 h p.i.).

## INTRODUCTION

The capability of atomic force microscopy (AFM) (Binnig et al., 1986) to operate at very high resolution in a liquid environment (Marti et al., 1987; Drake et al., 1989), even with atomic resolution in liquids through repulsive and attractive forces (Ohnesorge and Binnig, 1993) offers a great potential for the research in the biochemical and biological or biomedical fields. Biological specimens can be studied by AFM in their natural aqueous environment at a resolution of a few nm, in some cases obtaining even better results than electron microscopy [Hoh et al., 1991, 1992; Butt et al., 1991; Ohnesorge et al., 1990, 1992; Karrasch et al., 1993, 1994; Yang et al., 1993; Schabert et al., 1995 (for an overview see, e.g., Hoh et al., 1992; Hansma and Hoh, 1994)]. Moreover, AFM opens the exciting possibility of investigating the kinematics of biological processes down to the molecular scale as first presented by Drake et al., 1989. More recently, detecting enzyme activity by AFM directly was reported (Radmacher et al., 1994). Häberle et al. (1991) have been the first to show the capability of the AFM to, in principle, investigate and image the wall of a single living cell that was held by a micropipette. Butt et al. (1990) imaged living plant cells. Processes observed on the membrane of pox-infected monkey kidney cells, including the exocytosis of a virus particle, have been reported in Häberle et al. (1992) and Hörber et al. (1992). Several groups have

*Received for publication 31 October 1996 and in final form 16 May 1997.*

Address reprint requests to G. Binnig, IBM Research Division, Zurich Research Laboratory, Säumerstrasse 4, CH-8803 Rüschlikon, Switzerland.

Dr. Ohnesorge's present address is Dept. of Engineering, University of California, Santa Barbara, CA 93106.

Dr. Hörber's present address is EMBL, Meyerhofstrasse 1, D-69117 Heidelberg, Germany.

Dr. Häberle's present address is IBM Research Division, Zurich Research Laboratory, Säumerstrasse 4, CH-8803 Rüschlikon, Switzerland.

Dr. Smith's address is Sloan School of Business, MIT, Boston, MA.



0006-3495/97/10/2183/12 $2.00

investigated processes on living cells by AFM, where in most cases the cells were deposited on flat solid substrates; more AFM work on cells can be found [Henderson et al., 1992 (glial cells); Radmacher et al., 1992 (human platelets); Kasas et al., 1993 (cultured lung carcinoma cells); Hoh et al., 1994; Schoenenberger and Ho, 1994 (MDCK and R5-cells); Lal et al., 1995; Shroff et al., 1995 (rat myocytes and fibroblasts); Braunstein and Spudich, 1994; Spudich and Braunstein, 1995 (RBL-cells)]. A temperature-controlled AFM experiment on cells was attempted (Häberle et al., 1995).

Here, we used the same biological system as Häberle et al. (1992) and Hörber et al. (1992). Our familiarity with its behavior allowed us to optimize and further explore the capabilities of the existing instrumental setup. The background information on the pox viruses is partly based on literature back to 1972, and is summarized from those articles in brief and incompletely here as far as is needed for interpreting the data. Pox (vaccinia) viruses [for an overview see, e.g., Moss (1986), Morgan (1976), Sodeik et al. (1994), Czerny et al. (1994)] are large DNA viruses (diameter of ~200–400 nm) and very complex in terms of their structure (Moss, 1986). The reproductive cycle as described in the literature [e.g., Payne and Kristenson (1979, 1982), Ichihashi et al. (1971), Stokes (1976), Blasco and Moss (1991, 1992), and C.-P. Czerny, privileged communication, Habilitationsschrift (1991)] can vary concerning the duration of different stages of maturation, depending on the kind of cells that are infected.

In our case of cultured monkey kidney (MK) cells as a host system, maturation of the first form of pox progeny virions, the so-called INV (intracellular naked virus enveloped by a double lipoprotein membrane) inside the cell is completed ~6 h after the infection [postinfection (p.i.)] (see Payne and Kristenson, 1979) for the very similar system of rabbit kidney (RK) cells. Roughly >10 h p.i. ~1–15% (MK cells) of all these virus particles have been wrapped into an additional double lipoprotein envelope at the Golgi apparatus, enabling them to actively leave the still-living cell via exocytosis (also referred to as "reverse phagocytosis," Payne and Kristenson, 1979; Ichihashi et al., 1971). That is, by fusion of their outermost envelope with the cell membrane, which initiates the exiting of the virions, they lose one of their extra envelopes, resulting in the so-called enveloped extracellular virus (EEV). Only a few percent of a total of ~1000 progeny virions are actively expelled by the still-living cell, whereas the remaining virus particles (INV and those already having the extra double envelope) are disseminated after rupture of the cell (C.-P. Czerny, privileged communication). The peak of the exocytotic events that release progeny virions from the living cells is reported to be ~16–20 h p.i. (Stokes, 1976).

In our AFM experiments on virus particles deposited on solid substrates we investigated them in water as well as in buffer solution. The INV is the most sturdy type of the vaccinia virus (Czerny and Mahnel, 1990); it is stable in a wide range of ambient conditions as opposed to the enveloped forms, especially the EEV, which lose their extra envelopes easily in inappropriate environments.

One of the keys to understanding viral infection is obviously the proteins on the viral surface. Many membrane proteins of vaccinia viruses have been identified and isolated [(for an overview see Sodeik (1992) and Czerny et al. (1994)]. For instance, two membrane proteins have been found to be directly related to viral infectivity of the INV form: a trimeric 14-kD so-called fusion protein (Doms et al., 1990; Rodriguez et al., 1986) and a 32-kD so-called adsorption protein, playing a crucial role in early virus-host interactions (Maa et al., 1990).

Other detailed structures on the viral surface, described in the literature as the so-called "surface tubules" apparently formed by a 54–58-kD tubular protein, were also found to be responsible for adhesion to the cell (Stern and Dales, 1976; Doms et al., 1990; Rodriguez et al., 1986). These molecular structures have been investigated by electron microscopy in isolated form (Stern and Dales, 1976; Sodeik et al., 1994) as well as on freeze-dried virus preparations where they predominantly cover the viral surface (Medzon and Bauer, 1970). On the surface of INV their diameter was found to be ~7 nm, and their length 40–45 nm (Stern and Dales, 1976; Medzon and Bauer, 1970). However, the diameter may vary depending on the preparation method; it was found to be about a factor of two to three larger for isolated tubules compared to those on intact viruses (Stern and Dales, 1976).

Investigating a single virus-infected living cell by AFM (see also Häberle et al., 1992; Hörber et al., 1992), especially when achieving a very high imaging rate, promises to deliver significant information on the processes that occur in the cell membrane during viral infection and maybe about the effects of specific drugs on an almost molecular scale. This is not possible at the moment with any other technique. However, mere imaging—lacking all information on many mechanical properties in the frequency range discussed here—can be speculated to be possible optically in the near future with comparable re-solution using new developments in video microscopy technology. Results obtained with current capabilities of this technique are indicated in the work of Cudmore et al. (1995) on vaccinia-infected cells, where other comparisons with our work can also be drawn.

Mechanical properties of cells are highly interesting in general and, perhaps, also with respect to viral infection. Preliminary experiments (on uninfected MK cells) in this direction are shown here, where the pipette was driven in the $z$-direction and the lever response detected with a lock-in amplifier; in many respects this follows the initial concept of tapping at low frequencies as suggested by McClelland et al., 1987, Digital Instruments, 1991, as well as the measurements presented in Radmacher et al. (1992, 1993).

Furthermore, frequency spectra of living cells were recorded showing mechanical resonances that could perhaps be specific for the cells used, but not necessarily (see Note 1); which, if it can be proven to be true, may have important

applications in the medical field concerning the treatment of viral diseases and cancer. In some aspects, these data are related to the findings of Zemann et al. (1990) or Strey et al. (1995) concerning what they call "cell flickering."

## MATERIALS AND METHODS

The AFM used for the investigations of pox viruses on a solid substrate [thermally oxidized silicon wafers (Note 2)] has been described in Ohnesorge (1994); the AFM for imaging single living cells held by a micropipette mounted on the scanner-piezo has been described in Häberle et al. (1991, 1992, 1995) and Hörber et al. (1992), and is sketched schematically in Fig. 7–0. Both instruments use the well-known optical beam deflection method (Meyer and Amer, 1988; Alexander et al., 1989) to detect the force sensor motion. The imaging forces are estimated to be $\sim 10^{-10}$ N. Using the "pipette-AFM" configuration (Häberle et al., 1991, 1992; Hörber et al., 1992) allows a very fast scanning speed for imaging cells in the variable deflection mode, most reliably when using optical detection of the cantilever motion, since the parts moving in the liquid—the cell itself and a short portion of the thin end of the scanning pipette—are very small; therefore, in contrast to the standard procedure of imaging cells adsorbed to a large flat substrate on the scanner stage, no significant excitation of disturbing waves or convection in the liquid occurs, or at least to a far lesser extent. Additionally, the severe deformation of the cells, which occurs when adsorbing them onto a solid substrate, is avoided. However, it has to be noted that there is a significant discrepancy between forward and backward scan lines in the form of a rather strong phase shift between both traces, which is not surprising at those very high scan rates of one frame in 1–3 s due to the elastic properties of this specific setup. The temperature of the liquid bath in which the cells were imaged was ~25–30° C, i.e., somewhat below normal body temperature. Therefore, all processes observed may be somewhat slowed compared to the normal physiological case.

For measuring mechanical properties of cells, very stable imaging conditions were required at an extremely slow scan rate of ~1 frame in 5 min. The curvature of the cell was compensated for by using the second-order slope correction: the 90°-phase-shifted, rectified, and low-pass-filtered regular slope correction signal is additionally added to the piezo voltage controlling the $z$-position of the sample. Here, the low-pass filter removes high-frequency contributions of the correction signal due to the rectification in order to avoid mechanical resonances ("ringing") of the scanner unit, particularly at higher scanning rates. By adjusting the amplitude of this correction signal and the time constant of the low-pass filter, the correction signal can roughly be fitted to the curvature of the cell. For the very rapid scan images shown here, this second-order slope correction was not applied. An Arlunya A/D-D/A processor recorded the image data (Note 3). We used commercially available (Note 4) $Si_3N_4$ cantilevers with integrated tips that had been metal-coated (e.g., 100–200 Å Au on 10–20 Å Cr). The coating appeared to reduce friction effects in some cases, particularly at high scanning rates.

Virus particles (orthopox, strain Munich1 or Elstree (Czerny and Mahnel, 1990) were deposited from purified suspension onto poly-L-lysine-coated $SiO_2$ substrates [thermally oxidized silicon wafers, oxide layer thickness ~150 nm (Note 2) to investigate their structure by AFM in buffer solution (PBS, pH 7.2–7.4] or water. Virus production and purification has been described in detail elsewhere (Czerny and Mahnel, 1990). During imaging, the living (see Abstract and Note 5) cultured monkey kidney cells (Microbiology Associated, MA-104, diameter ~15 $\mu$m) were kept in their standard growth medium (EMEM, Czerny and Mahnel, 1990), the pox viruses infecting the cells (strain Munich1 or Elstree, titer $10^7$K/D50/ml, size 200–400 nm) were suspended in the same solution.

## RESULTS AND DISCUSSION

### Viruses

The viruses were found in clusters (Fig. 1, *a* and *b*) or as single particles (Fig. 1 *e*) on the substrate, as is well familiar from scanning electron microscopy (SEM) images (C.-P. Czerny, privileged communication). The high-magnification image (Fig. 1 *c*) of one of the virions in Fig. 2 shows a

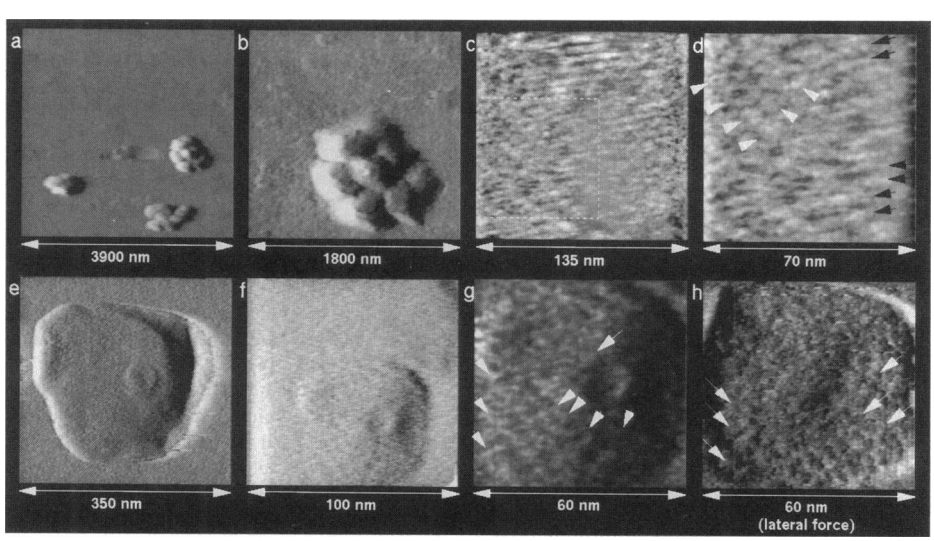


FIGURE 1 Image series with different magnifications of pox viruses recorded in water (*a–d*) and in buffer solution (*e–h*). (*c*) is taken on the virion in the center of the cluster of eight virus particles in (*b*). (*d*) A close-up [same data as (*c*), only enlarged print] of the region indicated in (*c*). In (*c*) and (*d*) lamellar structures and in the left-hand half of the frame a quasi-ordered region of spherical or ringlike structures (diameter ~5–10 nm, sometimes up to 15 nm) are observed. The white arrowheads in (*d*) indicate the spherical or ringlike structures (in some cases even subunits seem to be visible) in the quasi-ordered region. The black arrows point in the direction of the lamellae or tubular structures. (*e* and *f*): Different magnifications on a single virion in buffer solution, which we believe to be one of the enveloped forms (EEV). The origin of the 60-nm spherical structure on the virion is not known. In all images, when quantifying the apparent resolution, multitip effects may have to be considered owing to an elasticity of the viruses. These effects are probably very significant in (*e* and *f*), whereas in (*c* and *d*) they are most likely negligible.

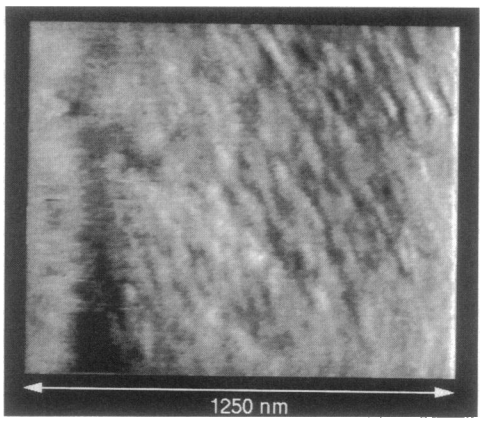


FIGURE 2 Uninfected MK cell imaged in vitro in aqueous solution at a scan rate of ~15–20 s per frame with an apparent lateral resolution of ~15 nm. Quasi-periodicities are probably strongly influenced by multiple tip effects.

lamellar structure. Fairly regularly repeating pairs of rod-shaped structures with a total width of ~7–11 nm and a length of ~60–90 nm are seen. On the left-hand side of the image, quasi-ordered patches are visible consisting of units with a diameter varying from 5 to 10 nm, in a few cases up to 15 nm, which exhibit a ringlike shape in a few cases (Fig. 1, *c* and *d*). Fig. 1 *d* is an enlarged view of the region as indicated in Fig. 1 *c*; Fig. 1, *c* and *d* are taken from one and the same image scan, i.e., they represent the same data, containing the most detail; all other images are separate scans. Fig. 1, *e* and *f* show a series of images of a single particle, which we suppose is one of the additionally enveloped forms of the vaccinia virus (EEV or the doubly enveloped intracellular form) suggested by its much softer appearance than for the particles in Fig. 1, *a–d*, which we therefore interpret to be the INV; this is plausible because the viral suspension can contain all forms of virions, INV, EEV, and the intracellular intermediate, although many fewer of the enveloped forms (C.-P. Czerny, privileged communication).

The pairs of lamellar, rodlike objects (Fig. 1 *c*, partly also Fig. 1 *d*) probably represent the surface tubules due to the agreement in appearance and size with the electron micrographs in Stern and Dales (1976) and Medzon and Bauer (1970). The ringlike structures and ordered units may possibly represent top views of such tubular protein structures at the edge of the virion (Fig. 1, *c* and *d*) but they could be due to other molecular scale details as well. Owing to the elasticity of these fairly large virus particles, one has to consider multiple tip effects, which, in Fig. 1, *c* and *d*, very likely cause periodic structures to appear exaggerated. For comparison, Karrasch et al. (1993) show impressive submolecular resolution by AFM on the hard crystalline bacteriophage T4 polyhead.

The origin of the circular structures in the single particle in Fig. 1, *e–h* is not known to us. It could be vaguely speculated that it is related to the closing of the envelope when the INV is being engulfed by an additional membrane at the Golgi apparatus (Sodeik et al., 1994; Stolz and Summers, 1972; G. Griffith, privileged communication; for some detail on the early virus maturation, see also B. Sodeik, 1992) or it might have to do with a structure seen on the particle adhering to the cell in Fig. 3 *B*, and thus possibly even with the mechanism for transporting the progeny virions along the cytoskeleton inside the cell and/or the passage of the cell wall. Preliminary experiments with gold-labeled monoclonal antibodies have been attempted but have not yet yielded presentable results.

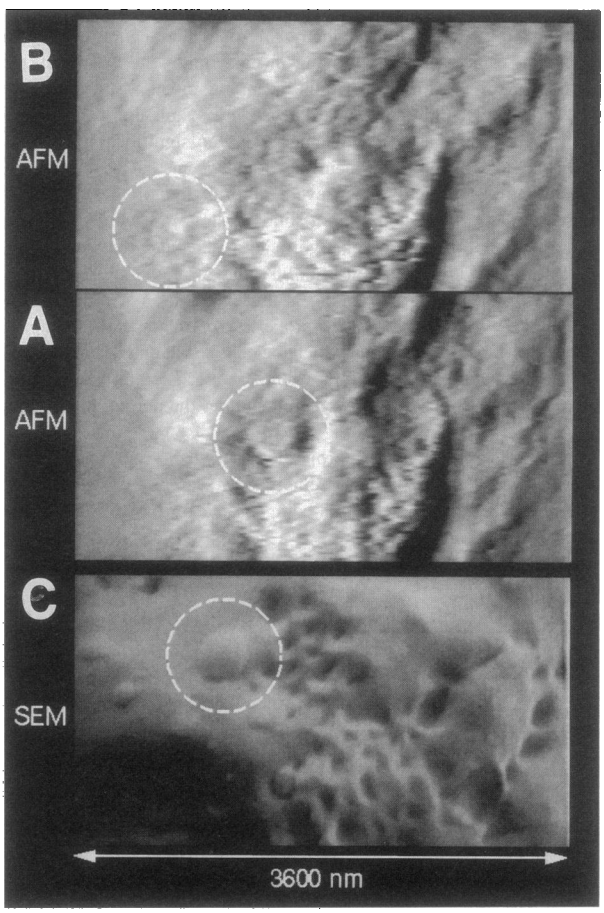


FIGURE 3 (*A* and *B*): AFM images of an infected cell taken in aqueous solution ~19 h after incubating the cells with virus particles. The spherical protrusions indicated most likely represent virus particles attached to the cell (perhaps just "cell-associated viruses"). Some internal structures may also be visible. (*B*) was recorded ~20 min. after (*A*). (Scan window 3.6 × 3.0 $\mu m^2$, scan speed 3 s per frame). We do not know (*B*) the origin of the dumbbell-shaped detail attached to the spherical particle most likely representing a virus on or within the cell wall. It almost appears in shape like the heads of a myosin molecule, which may not be too unlikely considering that the virions are actively transported along the cytoskeleton inside the cell (Moss, 1986). Perhaps there is a relation to the circular structure seen in Fig. 1 (*e* and *f*). (*C*): Low-voltage SEM image (recorded by H. G. Liebich, Note 6) of the surface of a virus-infected cell, which was fixed with glutaraldehyde but otherwise unstained. The appearance of the area on the cell is very similar to the AFM images.

## Virus-infected living cells

A suspension of MK cells was incubated with a large amount of viruses (~10–100 viruses per cell). Imaging with AFM in the variable deflection mode on a single cell held by a micropipette (aperture ~5 μm) was begun ~14 h after the incubation. Over a scan size of 3.6 × 3.0 μm a scan rate of as little as one frame per second still allowed a lateral resolution of 30–40 nm. For smaller scan sizes and at slower scan rates an apparent resolution as small as ~10–15 nm could be obtained, where again multiple tip effects certainly have to be considered. This is shown in Fig. 2, where an uninfected MK cell has been scanned at ~1 frame in 15–20 s.

The cells did not look significantly different shortly before and after infection. Noninfected cells seem to appear slightly softer on an overall scale than those that have been infected for many hours. Since in this case there was no noticeable variation of neither structural details nor overall softness upon infection [in contrast, which is still completely unclear to us, to some earlier observations (Häberle et al., 1992)] and because the chance that a virus would enter the cell just underneath the scanning tip probably was negligible, we changed the experiment to using pre-infected cells, which abbreviated each experiment by ~10 h.

According to Blasco and Moss (1991, 1992) and Payne and Kristenson (1982) many virions remain adsorbed to the cell surface and never enter the interior; progeny virions are also known to stay attached to the cell wall on the extracellular side after they have exited through the membrane. Fig. 3, *A* and *B* show the surface of the infected cell as seen by the AFM ~19 h after the incubation. The contrast disappears toward the side-edges of the frames, because here the curvature of the cell has not been compensated for and because imaging is done in the variable deflection mode; thus the loading force decreases toward the side-edges of the frame. In the SEM image in Fig. 3 *C*—recorded by H. G. Liebich (Note 6)—with low-voltage SEM on glutaraldehyde-fixed but otherwise unstained samples, a very similar region of the surface of an infected MK cell is visible; the spherical protrusions are generally believed to represent adsorbed virus particles (C.-P. Czerny, H. G. Liebich, privileged communications). Therefore, the spherical protrusions indicated in the AFM images (Fig. 3, *A* and *B*) ~300–400 nm in size, most likely also represent such adsorbed virus particles [("cell-associated viruses"—Blasco and Moss, 1991, 1992; Payne and Kristenson, 1982)] as seen with the AFM on a living cell. Fig. 3, *A* and *B* show the same region of the cell ~20 min apart, while the cell was continuously being scanned at a rate of ~3 s/frame. The objects in Fig. 3, *A* and *B* were visible for only a few minutes. A mechanical influence of the tip, which exerts the highest force in the middle of the frame, seems very likely. In Fig. 3 *B* more contrast is visible on the left-hand side of the frame owing to an increase of the loading force and slope correction. The apparent "dumbbell"-shaped object across the spherical particle in Fig. 3 *B* is absolutely not yet understandable to us, if it is a real structure at all, since we observed it only once. It almost looks like a "molecular hinge" of "myosin head" shape and size attached to the supposed virion, and can perhaps be related also to the circular structure visible on the particle in Fig. 1, *e* and *f*, as well as to a similar detail (as in Fig. 1, *e* and *f*) slightly visible on the supposed virion in Fig. 3 *b*, where no such "dumbbell" can be seen. This would support the suggestion that the object in Fig. 1, *e* and *f* is an EEV, i.e., a particle that had actively been expelled by a cell when it was still living. Since pox progeny virions are known to be actively transported along the cytoskeleton inside the cell (Moss, 1986), it may actually seem not too unlikely to find myosin heads attached to the viruses.

The protrusions in Fig. 3, *A* and *B* were reproducibly visible in several scans but were only seen in this experiment so clearly; they partially disappeared after a few minutes and we cannot say whether this was due merely to a destructive mechanical tip influence or to real cellular activity. Including earlier measurements (Häberle et al., 1992; Hörber et al., 1992), large (>100 nm) spherically shaped particles of roughly virus size (200–400 nm) were observed on some infected cells, in total roughly half a dozen times. We never saw large particles of this kind on uninfected cells, only much smaller ones (more than one order of magnitude smaller).

An enhanced activity of virus-infected cells is apparently indicated in the AFM observations by a significantly pronounced activity in their membrane. The scan speed for imaging the sequence in Fig. 4 was ~1 frame/s. Parts of the images changed drastically while other areas remained absolutely stable. The process in Fig. 4 was observed ~18 h after the cells had been incubated with the virus suspension and possibly represents the rearrangement of parts of the cytoskeleton. It should be noted that the mechanical influence of the tip on the structural changes seen in Fig. 4 probably plays an important role in this case of a very rapid change from one frame to the next.

Fig. 5 (equivalent to Fig. 4f published already in Hörber et al., 1992—same data as here) most likely shows a transport process (possibly of viruses) along or slightly underneath the cell surface observed ~24 h after incubation. From Fig. 5 (or Fig. 4f in Hörber et al., 1992) the transport velocity along the membrane is estimated to be ~0.1–0.2 μm/s. It should be noted that AFM always measures a convolution of local topography and local elasticity; therefore, especially when imaging cells, it is very often not clear whether the structures seen represent the surface topography or locally varying elasticity slightly underneath the surface. For instance, it is known (Moss, 1986) that progeny virus particles are transported along cytoskeletal structures inside the cell. Such a process occurring slightly underneath the cell membrane may perhaps be indicated in Fig. 5. A possibility of distinguishing between tip-induced and real cellular kinematic effects would be simply by varying the loading force or by using AC-imaging modes, as indicated in Fig. 8 or as shown in Radmacher et al. (1992).

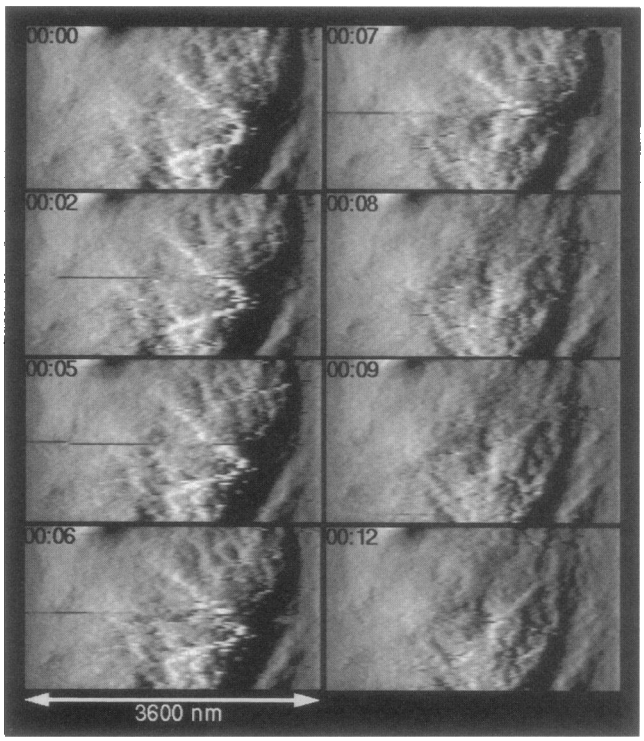


FIGURE 4 $3.6 \times 2.0\ \mu m^2$ scan of an infected cell in aqueous solution, scan rate ~1 s per frame. The time elapsed is indicated on each frame in min/s. A filamentous structure appears to change rapidly, although a mechanical influence of the imaging tip cannot be ruled out. All images are complete scan frames, except the frame marked with 00:07, for which the vertical scan has proceeded until the middle of the frame (from bottom to top); i.e., this is merely the upper half of the previous frame and the lower half of the next frame for better visualization. Hundreds of scan frames before and after the sequence shown were recorded reproducibly at the same imaging rate, continuously showing the same appearance except for variations of small details in the image.

Several mechanisms by which host cells release viruses are widely known, such as so-called "budding" or exocytosis using vesicles or coated pits [see, e.g., Fields and Knape (1986)]. Although pox viruses use a very specialized mechanism, regular budding, even though considered very unlikely, has not absolutely been ruled out in the literature (Tsutsui et al., 1983; Ichihashi et al., 1971; Griffith, privileged communication). [Note: Tsutsui et al. report the observation of budding of vaccinia viruses from FL cells; however, they and Ichiashi et al. state that there is no evidence for budding from RK-13 cells.]

The literature describes two release mechanisms as known from electron microscopy (e.g., Blasco and Moss, 1991, 1992; Payne and Kristenson, 1982; 46), which differ largely in structural appearance on the scale of the size of a virus, whereas the principal mechanism of exiting through the cell membrane may be more or less the same. Stokes (1976) describes high-voltage electron microscopy data showing the release of progeny virions at the end of specialized microvilli (Stokes, 1976; Krempien et al., 1981), showing striking similarity to the AFM observation reported in Häberle et al. (1992) and Hörber et al. (1992). Payne and Kristenson (1979) and Ichihashi et al. (1971) explain in detail the release mechanism of progeny virions via the additionally double-membraned intermediate virus type inside the cell as observed by electron microscopy on thin-sectioned cell preparations. By fusion of the outermost viral envelope with the cell membrane from inside the cell the EEV is expelled, leaving a depression in the cell membrane. The electron micrographs of thin sections of infected cells in Payne and Kristenson (1979) and Ichihashi et al. (1971) have convincing parallels to the AFM data shown in Fig. 6. At a scan rate of ~1 frame every 3 s the evolution of a protrusion at the lower end of the images can be followed. In each frame in Fig. 6, the elapsed time has been indicated in min/s. A large protrusion (~>200 nm) slowly becomes visible (00:00–01:09) and its appearance seems to vary in a pulsating manner (01:11–01:20 and 04:19–05:27). Also, for ~2 min (05:31–07:33), a small (<100 nm) additional protrusion next to the large original one is visible; its appearance seems to correspond to protrusions that are often seen in TEM images (e.g., Ichihashi et al., 1971). A similar observation was already shown in Häberle et al. (1992). Possibly these even have the same origin as the "molecular dumbbell" in Fig. 3 *B*. At roughly the same time, the large protrusion begins to increasingly grow out of the membrane (07:30–08:45). Between 08:03 and 08:17 the image frame has been shifted slightly upward. Beginning at 08:51, the further-growing protrusion begins to lose lateral stability. Finally, ~9 min after its first appearance, the protrusion suddenly disappears, leaving a depression of ~300–400 nm diameter in the cell wall. The strong distortion to the left of the disappearing protrusion and the shadowing effect appearing on the left-hand side of the depression in the cell membrane is due primarily to lateral force effects at a fast scan direction from right to left. The other two structures in the middle and in the upper left of the frame certainly acquire their triangular shape from the same distortion. However, their appearance does not change with time; it depends only on the loading force. This is seen, for instance, by comparing frames −00:07–00:59, in which the contrast is low due to a relatively small loading force with the frames 05:37–07:47 at slightly higher forces. On the other hand, the protrusion, which we believe is a virus, drastically changes its appearance beginning at 08:51, while nothing else in the images changes, which indicates a stable constant imaging force. Therefore, we concluded that the particle was actively expelled by the cell. Imaging force variation would change the contrast throughout the image. Nevertheless, a mechanical influence of the imaging tip on this process cannot be ruled out completely here either, but it most likely does not, in principle, alter the process in this case.

This exocytotic event is convincingly similar to the top-view appearance of the release mechanism described in Payne and Kristenson (1979) and Ichihashi et al. (1971) based on the cross-sectional information of the transmission electron micrographs.

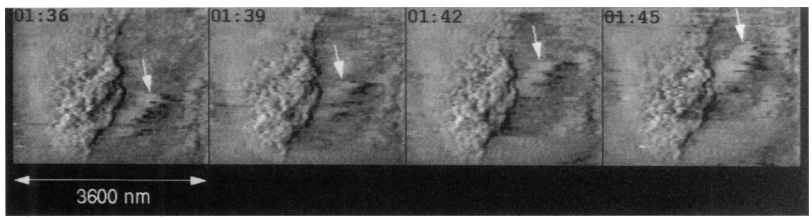


FIGURE 5 This measurement has already been published earlier in Hörber et al., 1992, where the equivalent image (recorded roughly a couple of minutes before the sequence shown here) may be also viewed in their Fig. 4f. 3.6 × 3.0 $\mu m^2$ scan on an infected cell, scan rate ~3 s/frame. The time counter on each frame reads min:s. Several structures are continuously moving along the cell membrane, perhaps also slightly underneath. The velocity of the objects is ~0.2 $\mu$m/s, in Fig. 4f of Hörber et al. 1992, about half of that.

In summary, we believe that we have also (as referred to the earlier report in Häberle et al., 1992) here most likely observed the release of a virus particle for the following reasons:

1. The contrast of the particle gradually varies while nothing else in the image field changes during many consecutive frames. This accounts for the particle being actively expelled by the cell as opposed to imaging-force-

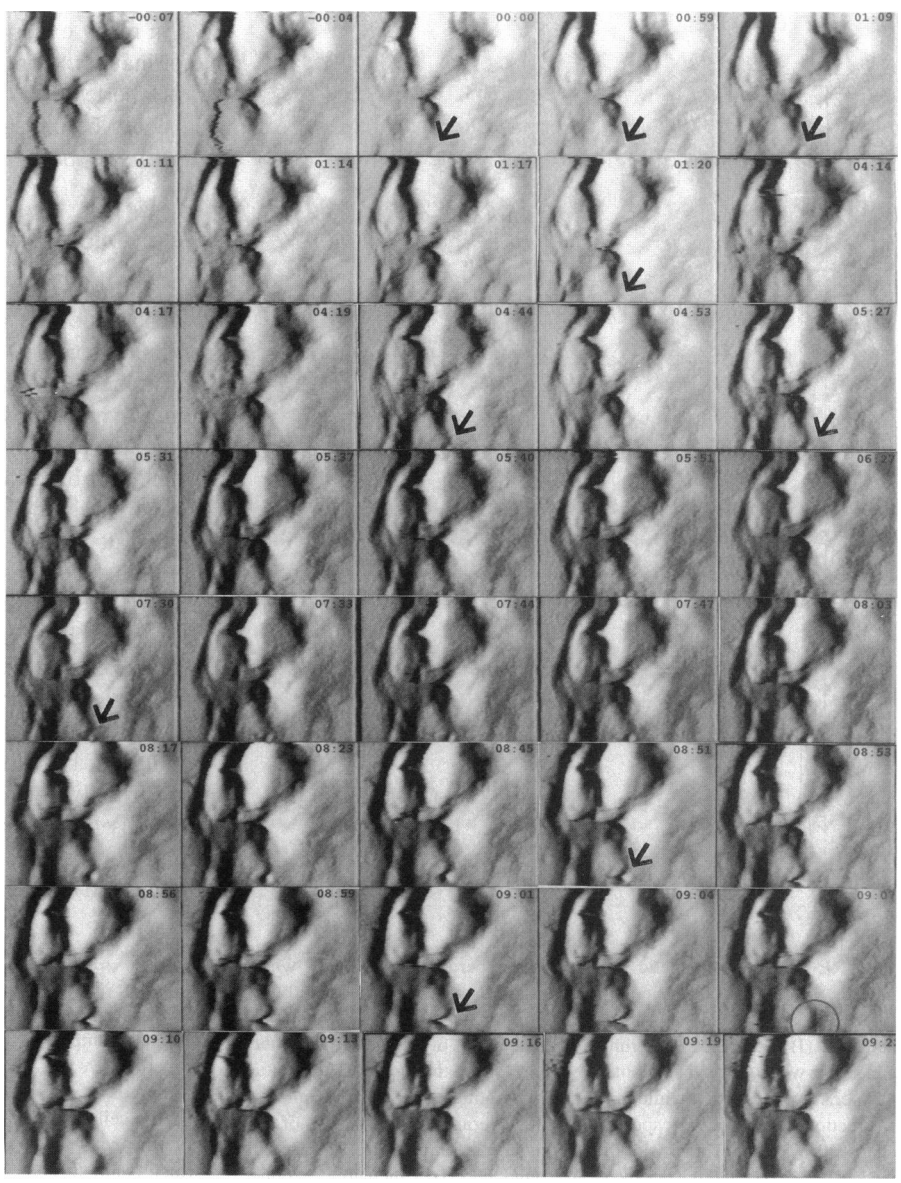


FIGURE 6 3.6 × 3.0 $\mu m^2$ scan, 3 s/frame. A protrusion (~200 nm in size) appears at the bottom of the frames (00:00–01:09) and starts to grow out of the cell membrane. About 9 min after its first appearance, the protrusion suddenly (09:07) disappears leaving a depression (~400 nm in diameter) in the cell membrane. This process most likely represents the exocytosis of a virus particle. The strong distortion of the disappearing particle and the distorted appearance on the left-hand side of the depression are due to lateral force and phase shift effects at a scan direction from right to left.

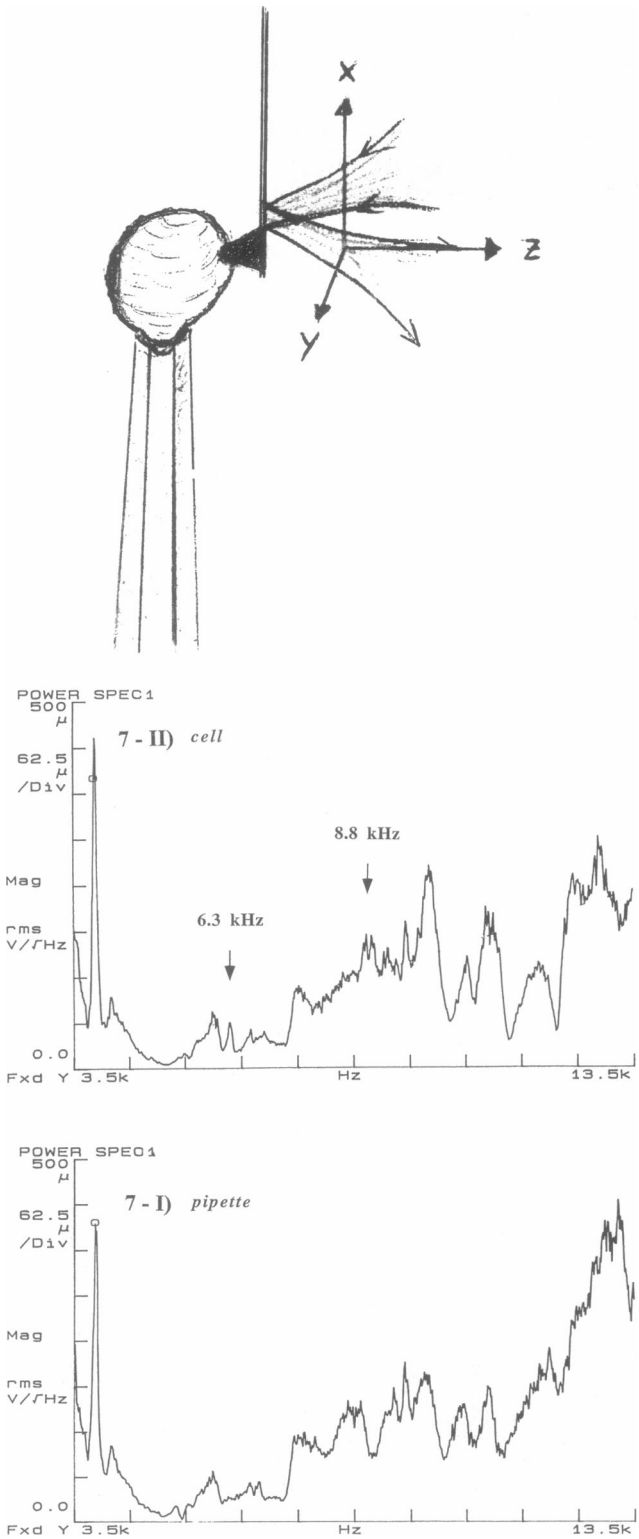


FIGURE 7 (0): Schematic sketch of the experimental geometry when holding the cell with the scanned pipette against the cantilever tip with the illumination indicated as well as the coordinate system for the piezo actuator. (I) Frequency spectrum (scaled average of 100 spectra) of the cantilever when the tip is in contact with the end of the pipette. The pipette has been excited with a white noise signal amplitude of ~6 nm rms in the z-direction. (II) Frequency spectrum (scaled average of 100 spectra) of the cantilever when in contact with the cell, otherwise same as for (I). Note the peak at ~6.3 kHz and the double peak around 8.8 kHz, which are not found in (I). They could perhaps constitute very interesting viscoelastic properties of the cell, although the possibility of them being an artifact cannot yet be ruled out completely (Note 7). We note further that even if the experimental parameters (e.g., lever position near the cell) do not strongly affect the measurement, these peaks here may still not be characteristic for the specific cell-type used, although they could be, but could be dominated by both the cytoskeletal architecture and simply the size/geometry of the cell, which could still be extremely interesting.

variation-induced contrast changes, which would affect all structural details almost equally. Many consecutive scan frames are needed at a very rapid imaging rate in order to be able to distinguish between those two effects, and this is sufficiently achieved here.

2. The event was observed 20 h after the cells had been incubated with highly concentrated virus suspension; this is roughly the time span after the infection after which the highest probability of virus release is to be expected (Czerny, privileged communication; Stokes, 1976).
3. The size of the released particle corresponds to the size of a virus.
4. The appearance of the process matches well the description of the release mechanism described in Payne and Kristenson (1979) and Ichihashi et al. (1971), and the general picture of exocytosis via membrane fusion ("reverse phagocytosis").
5. Such characteristic exocytotic processes releasing such large particles were never observed on noninfected cells in many experiments during many hours of observation.
6. Finally, the process looks further very similar to Fig. 9 in Haberle et al. (1992), meaning that both observations could be the same biological process of a virus particle actively being expelled from the cell.

## Mechanical properties of the MK cells

Force microscopy requires the sample under investigation to withstand locally applied imaging forces, which here were on the order of $10^{-9}$ to $10^{-10}$ N (estimated). Seemingly the mechanical rigidity of the cells is sufficient for AFM imaging, which is by no means obvious at all. Therefore, we attempted to quantify mechanical properties of the MK cell when held by a micropipette mainly using the well-known force modulation technique mentioned, for instance, in Binnig et al. (1986), McClelland et al. (1987), or applied to biological samples in Radmacher et al. (1992, 1993). However, here we were particularly also aiming for spectral resolution. The pipette-AFM concept (Häberle et al., 1991) should be very well suited for these kinds of experiments because, as mentioned above, perturbation by excitation of convection or waves in the liquid by the scanning parts should be, by comparison, extremely small, although they are certainly not completely negligible, either. Furthermore, the cells held by a pipette supposedly are in a state much more comparable to that of a cell freely suspended in a liquid than a cell adhering onto a substrate.

To characterize the experimental setup, frequency spectra were taken first. Fig. 7, I and II show the frequency spectrum (Note 7) with the imaging tip in contact with the cell (curve II) and the reference spectrum with the tip in contact with the very end of the pipette (curve I), respectively. In both cases, the pipette was excited in the $z$-direction (see schematic sketch Fig. 7–0) with a white noise signal applied to the piezo corresponding to an amplitude of ~6 nm rms. The spectra clearly coincide except for a resonance at 6.3 kHz and a double peak at ~8.8 kHz; above 10 kHz the amplitudes in curve I and II start to deviate strongly from each other, but the frequency position of peaks roughly remains the same. These resonances may perhaps simply originate from the direct coupling between pipette and cantilever directly through the liquid, which is different in the cases of curve I and II due to slightly different geometry, meaning that they are possibly a complicated artifact (Note 7) which, however, may be unlikely (for properties of cantilevers vibrating in a liquid see Schaeffer et al., 1996). More interestingly, however, these resonances could perhaps originate from the cell itself or from the springiness of its attachment to the pipette. This would constitute a rather surprising viscoelastic property of the cellular architecture. However, we emphasize that especially in the frequency regime investigated here, the size and geometry of the cell may have the dominant influence on the spectra here, rather than a characteristic cell-type-specific cytoskeletal architecture of smaller constituents, whose effects would have to be expected in much higher frequency regimes. We note also at this point that apparent resonance properties of cells (erythrocytes) had been described (Zemann et al., 1990; Strey et al., 1995), although in a very low frequency regime.

Fig. 8 *A* shows a constant force image of the cell. The maximum apparent height differences are ~30 nm. The apparent excess height of ~100–200 nm in the middle of the frame compared to the $z$-level at the sides caused by the cell's curvature has been compensated for using the second-order slope correction as mentioned above. Fig. 8, *B* and *C* record, respectively, the amplitude and phase signal of a lock-in amplifier (Note 8) on the same region on the cell surface when the $z$-position of the cell is modulated at 2 kHz with an amplitude of ~2 nm—corresponding to a force modulation of $\sim 10^{-10}$ N—and with the tip continuously in contact with the cell surface. Scanning was done in the constant force mode with respect to the mean deflection of the oscillating (2 nm/2kHz) cantilever, such that a possible influence of the cell surface topography is eliminated. As described in Radmacher et al. (1992, 1993) the amplitude response component of the lever approximately corresponds to the local elasticity, the phase signal (polar coordinates) to the viscosity. Fig. 8, *B* and *C* display the in-phase (with respect to the driving signal) amplitude and the $\pi/2$ out-of-phase signals, respectively, and contain different information from Fig. 8 *A*. A plateau-like structure appears to be visible, perhaps representing a "patch-like" or "mosaic-like" variation of local elasticity or viscosity of the cell membrane and the cell wall construction.

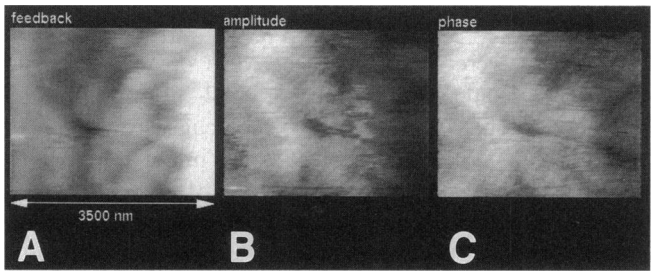


FIGURE 8 (*C*) Constant force ($10^{-10}$-$10^{-9}$ N) image of an uninfected living cell recorded in aqueous solution while the pipette is modulated with ~2 kHz and a 2-nm amplitude in the $z$-direction. The image size is ~3.5 × 3.0 $\mu$m, scan rate ~5 min/frame. The maximum apparent corrugations are ~30 nm. The overall curvature of the cell, which causes a height difference of roughly 100–200 nm between the center and the sides of the frame, has been compensated as described in the text. (*B*) and (*C*) force modulation images: (*B*) Amplitude signal from the lock-in amplifier (i.e., the signal output in phase with the reference) as the $z$ image signal of the same scan frame as in (*A*). The $z$-position of the cell is modulated at 2 kHz with an amplitude of ~2 nm; the response signal of the cantilever (contact-mode) provides the input for the lock-in, which is triggered with the 2 kHz reference. The mean (with respect to the modulation) deflection of the lever is kept constant by the feedback (i.e., constant force mode) to ensure that the loading force does not vary laterally, which could erratically influence the amplitude response of the lever. The amplitude image, which can be roughly regarded as an approximate measure of the local elasticity of the cell surface, seems to show a plateau-like structure. (*C*) as (*B*) the phase signal (i.e., the lock-in's signal output $\pi/2$ phase shifted with respect to the reference signal) roughly corresponding to local viscosity, is displayed, otherwise same as (*B*).

This experiment, in addition, for example, to those described in Radmacher et al. (1992, 1993), indicates that AFM may be able to provide quantitative information about the mechanical properties of a living cell. However, in order to derive reliable quantitative results on local elastic properties, these measurements have to be elaborated much further. The cytoskeleton supporting the membrane of a cell represents a very complex mechanical system, which may be able to react actively to externally applied forces (J. K. H. Hörber et al., "stretch channels", privileged communication). It is obvious to assume that local elastic properties of a cell are extremely frequency-dependent. The imaging measurement presented here provides only a qualitative statement on local elastic properties at 2 kHz. Furthermore, lateral force effects could contribute to the data, which should be recorded simultaneously to be able to separate the effects from the data.

For a thorough analysis of a cell wall elasticity map, one would have to record pixel-by-pixel a complete frequency spectrum of the cantilever response and derive image data in various frequency regimes. Furthermore, of course, one has to normalize the result with respect to the same system without the cell (as suggested in Fig. 7, as one also has to expect a frequency-dependent elastic response there, especially of the scanning pipette).

## CONCLUSIONS AND OUTLOOK

Pox viruses were investigated by AFM on the molecular scale with an apparent resolution of ~2–3 nm. Future experiments should aim to generate molecular scale maps of various viral surfaces, where proteins might possibly be identified by appropriate antibody or $F_{ab}$-fragment labeling or for small "hard" viruses simply by resolving the shape of the proteins (see Hoh et al., 1991, 1992; Butt et al., 1991; Ohnesorge, 1990; Ohnesorge et al., 1992; Karrasch et al., 1993, 1994; Yang et al., 1993; Schabert et al., 1995) or by combined local spectroscopy.

Living cells infected by pox virus were investigated with AFM—in some respect mainly reproducing earlier results (Häberle et al., 1992; Hörber et al., 1992) but now on a time scale of 1–3 s per image frame at a lateral resolution of 40 nm and a scan window of ~3.6 × 3.0 $\mu$m over time periods of many hours. Thus, hundreds of stable repeated scans of processes on the membrane of a living infected cell were recorded at a very fast imaging rate. We found that the exocytosis of a particle, which we believe to be a virus, through the cell wall takes ~9 min.

At present, such data, to our knowledge, cannot be achieved by any other technique; the authors believe, however, that improved purely optical microscopy techniques will, in the near future, allow a comparable imaging resolution including also the possibility for high-resolution movies (videomicroscopy), which would, however, then lack—in contrast to force microscopy—many important data on mechanical properties in the acoustic frequency range discussed here. A 100% direct proof of the expelled particle being a virus is still not available, because the unambiguous detection of the binding of monoclonal antibodies to the virus while it is being expelled would be extremely difficult, especially—among many other aspects—considering the rarity of these events. (Only about a few tens of virions are actively expelled by the still-functioning cell over a period of many hours).

Preliminary experiments to determine the mechanical resonance properties of living cells when held by a micropipette were performed by recording frequency spectra when the tip is in contact with the cell surface. A living cell held at the end of a micropipette seems to exhibit weak mechanical resonances in the regime of several kHz, which are most likely dependent—here perhaps even predominantly—on the cell's size and geometry as well as some experimental conditions (e.g., lever position near the cell). If we can prove such an effect [preliminary experiments were attempted in collaboration with V. T. Moy at the University of Miami (Note 1)], perhaps also at much higher microwave frequencies, to be cell-type-specific, this may possibly have significant implications in medicine. So far, as we want to emphasize at this point, this is mere speculation.

Maybe those mechanical resonances, if they exist, could then even be used to characterize cells and provide a kind of "spectroscopic fingerprinting" for intracellular structures and the effects of drugs on them; perhaps healthy cells will be distinguishable (see also Note 1 for additional attempts in that direction) from pathological ones (e.g., cancerous or virus-infected). Perhaps contagious cells could then be killed or passivated selectively by sharply driving certain resonances that would be specific for those sick and/or contagious cells only—perhaps in a much higher frequency range than studied here. Small virus particles might possibly exhibit similar, perhaps quite sharp, resonances too. Specific and selective narrow-band excitation of Raman-type modes in biomolecules or constructs thereof could perhaps prevent viruses from adhering to the target cells or simply mechanically destroy the viruses while running blood through a very high-Q tunable ultrasound or microwave resonator cavity. The possibilities are numerous but, however, we emphasize again most strongly that this is a mere speculation so far, as we have no idea about possibly drastic or even dangerous side effects of such a procedure which, of course, would have to be severely investigated and ruled out in an extremely reliable manner before being applied in therapeutics. Possibly, some empirical attempts for using a similar concept for medical treatment have already been made in the past elsewhere, however without using AFM; to date, the authors have not yet been able to find references on that.

Force modulation measurements like the ones shown here, but using much higher modulation frequencies (more than many MHz to microwave regime) may reveal qualitatively different new effects and insights, coming from a Raman spectroscopy or even optical spectroscopy point of view. Initial preliminary images of organic molecule films on solid substrates with AC-mode AFM in liquids at a lever vibration frequency on the order of 1 MHz (using regular commercial cantilevers) have been achieved already (Ohnesorge and Wong, 1996, unpublished results); the contrast formation is yet, however, completely nonunderstood.

## NOTES

1. Initial further experiments in this direction on living cells (a fibroblast cell line), deposited on a solid substrate, however, were performed very recently (1996) in a different laboratory in collaboration with V. T. Moy (who is hereby gratefully acknowledged) at the University of Miami. Other distinct effects on the acoustic regime frequency spectra of cells of similar nature were observed; here, treatment with chemicals or drugs seemed to change the frequency spectra recorded. These very preliminary measurements cannot rule out artifacts of the kind mentioned in (Note 7, 51) either, but they provided sufficient confirming confidence to mention the earlier findings in this report at all. Much more elaborate and thorough experiments have to be done, most likely using the pipette configuration, to prove these issues.
2. Wacker Chemie, Burghausen, Germany.
3. Image data were recorded with an Arlunya Model TF 5000 image processor (which provides a video signal output) with external control unit.
4. Park Scientific Instruments, Sunnyvale, CA 94089.
5. By the term "a living cell" we simply mean that the cell can still perform most of its functions; here it was "abused" to produce viruses. Note that it was a "tumor hybrid cell line" to begin with.
6. This SEM-image of an infected cell was recorded by H. G. Liebich, Veterinary Institute, University of Munich, using a JOEL625 at low e-beam voltages, where the specimens were fixed with glutaraldehyde, but otherwise unstained.

7. Although we believe this to be a real effect so far, these resonances might just be an artifact, because they could perhaps simply originate from the pipette-cantilever system, which is differently acoustically coupled to each other directly through the liquid in the cases of curve I and II. In both cases the lever might be excited through liquid waves generated by the vibrating pipette and the moving cell; due to the softness of the cell the lever may, also in the case of curve I, still be free to some small extent to oscillate, although of course strongly damped through the contact with the cell. However, we believe this to be rather unlikely, because besides those resonances, the spectra in curve I and II overlap rather well in terms of their qualitative shape. Furthermore, the excitation of the lever via convection or acoustics in the liquid caused by the very small portions of the vibrating pipette close to the lever and the moving cell itself should be extremely small (see also [54]) but maybe not negligible, which has not yet been clarified.

8. Spectra were recorded with a Hewlett-Packard HP 3562A spectrum analyzer, force modulation images with a Stanford Research Systems 530 lock-in amplifier.

We thank W. Oeffner for continuous help with and advice on electronics. We are very grateful to H. G. Liebich for recording the SEM image of virus-infected cells for Fig. 3 *C*. C.-P. Czerny and his assistants prepared cells, viruses, and buffers; provided articles, references, and background know-how from virology, and very informative discussions in respect to biology; they are acknowledged as well as B. Sodeik and G. Griffith. Furthermore, we are grateful for recent discussions of more general AFM aspects with members of the AFM group at the University of California, Santa Barbara (Hansma-Lab). V. T. Moy is gratefully acknowledged for providing the opportunity to perform further preliminary experiments in his laboratory at the University of Miami concerning mechanical resonance properties of cells and for his collaboration, also by giving advice in this respect with his expertise in biochemistry. We further thank L. M. Pavka for thorough English-language proofreading of the manuscript.

Present financial support to one of the authors (F.M.O.) through a Feodor-Lynen Fellowship from the Alexander von Humboldt foundation and a Honeywell corporation grant to P. Petroff's lab at UCSB is gratefully acknowledged.

## REFERENCES

Alexander, S., et al. 1989. An atomic resolution AFM implemented using an optical lever. *J. Appl. Physiol.* 65:164–167.

Binnig, G., C. F. Quate, and C. Gerber. 1986. Atomic force microscope. *Phys. Rev. Lett.* 56:930–933.

Blasco, R., and B. Moss. 1991. Extracellular vaccinia virus formation and cell to cell virus transmission are prevented by deletion of the gene encoding 37-kD outer envelope protein. *J. Virol.* 65:5910–5910.

Blasco, R., and B. Moss. 1992. Role of all associated enveloped vaccinia virus in cell to cell spread. *J. Virol.* 66:4170–4179.

Braunstein, D., and A. Spudich. 1994. Structure and activation dynamics of RBL-2H3 cells observed with SFM. *Biophys. J.* 66:1717–1725.

Butt, H.-J., E. K. Wolff, S. A. C. Gould, B. D. Northern, C. M. Peterson, and P. K. Hansma. 1990. Imaging cells with the atomic force microscope. *J. Struct. Biol.* 105:54–61.

Butt, H.-J., C. B. Prater, and P. K. Hansma. 1991. Imaging purple membranes dry and in water with the AFM. *J. Vac. Sci. Technol.* B9:1193.

Cudmore, S., P. Cossart, G. Griffiths, and M. Way. 1995. Actin-based motility of vaccinia virus. *Nature.* 378:636–638.

Czerny, C.-P., S. Johann, L. Hölzle, and H. Meyer. 1994. Epitope detection in the envelope of intracellular naked orthopox virus and identification of encoding genes. *Virology.* 200:764–777.

Czerny, C.-P., and H. Mahnel. 1990. Structural and functional analysis of orthopox virus epitopes with neutralizing monoclonal antibodies. *J. Gen. Virol.* 71:2341–2352.

Doms, R. W., R. Blumenthal, and B. Moss. 1990. Fusion of intra and extracellular forms of vaccinia virus with the cell membrane. *J. Virol.* 64:4884–4892.

Drake, B., C. B. Prater, A. L. Weisenhorn, S. A. C. Gould, T. R. Albrecht, C. F. Quate, D. S. Cannell, H. G. Hansma, and P. K. Hansma. 1989. Imaging crystals, polymers, and processes in water with the atomic force microscope. *Science.* 243:1586.

Fields, B. N., and B. M. Knape, editors. 1986. Fundamental Virology. Raven Press, New York.

Häberle, W., J. K. H. Hörber, and G. Binnig. 1991. Force microscopy on living cells. *J. Vac. Sci. Technol.* B9:1210.

Häberle, W., J. K. H. Hörber, F. Ohnesorge, D. P. E. Smith, and G. Binnig. 1992. In situ investigations of single living cells infected by viruses. *Ultramicroscopy.* 42–44:1161.

Häberle, W., D. P. E. Smith, J. K. H. Hörber, and C. P. Czerny. 1995. Proceedings of the Natick-Conference, 1995. In press.

Hansma, H. G., and J. Hoh. 1994. Biomolecular imaging with the AFM. *J. Annu. Rev. Biophys. Biomol. Struct.* 23:115–139.

Henderson, E., P. G. Haydon, and D. S. Sakaguchi. 1992. Actin filament dynamics in living glial cells imaged by atomic force microscopy. *Science.* 257:71944.

Hoh, J., and P. K. Hansma. 1992. Atomic force microscopy for high-resolution imaging in cell biology. *Trends Cell Biol.* 2:208.

Hoh, J. H., R. Lal, S. A. John, J. P. Revel, and M. F. Arnsdorf. 1991. AFM and dissection of gap junctions. *Science.* 253:1405–1408.

Hoh, J. H., J.-P. Revel, and P. K. Hansma. 1992. Membrane-membrane and membrane-substrate adhesion during dissection of gap junctions with the AFM. *SPIE.* 1639:212–215.

Hoh, J. H., and C.-A. Schoenenberger. 1994. Surface morphology and mechanical properties of MDCK monolayers by AFM. *J. Cell. Sci.* 107:1105–1114.

Hörber, J. K. H., W. Häberle, F. Ohnesorge, G. Binnig, H. G. Liebich, C. P. Czerny, H. Mahnel, and A. Mayr. 1992. Investigation of living cells in the nanometer regime with the atomic force microscope. *Scanning Microscopy.* 6:919–930.

Ichihashi, Y., S. Matsumoto, and S. Dales. 1971. *Virology.* 46:507–532.

Karrasch, S., M. Dolder, F. Schabert, J. Ramsden, and A. Engel. 1993. Covalent binding of biological samples to solid supports for scanning probe microscopy in buffer solution. *Biophys. J.* 65:2437.

Karrasch, S., R. Hegerl, J. H. Hoh, W. Baumeister, and A. Engel. 1994. Atomic force microscopy procedures faithful high-resolution images of protein surfaces in an aqueous environment. *Proc. Natl. Acad. Sci. USA.* 91:836.

Kasas, S., V. Gotzos, and M. Celio. 1993. Observation of living cells using the atomic force microscope. *Biophys. J.* 64:539.

Krempien, U., L. Schneider, G. Hiller, K. Weber, E. Katz, and C. Jungwirth. 1981. *Virology* 113:556–564.

Lal, R., B. Drake, D. Blumberg, D. R. Saner, P. K. Hansma, and S. C. Feinstein. 1995. Imaging real-time neurite outgrowth and cytoskeletal reorganization with an AFM. *Am. J. Physiol.* 269:C275–C285.

Maa, J. S., J. F. Rodriguez, and M. Esteban. 1990. Structural and functional characterization of a cell surface binding protein of vaccinia virus. *J. Biol. Chem.* 265:1569–1577.

Marti, O., B. Drake, and P. K. Hansma. 1987. AFM of liquid covered surfaces: atomic resolution images. *Appl. Phys. Lett.* 51:484.

Medzon, E. L., and H. Bauer. 1970. *Virology.* 40:860–867.

Meyer, G., and N. M. Amer. 1988. *Appl. Phys. Lett.* 53:1045.

Morgan, C. 1976. *Virology.* 73:43–58.

Moss, B. 1986. Replication of pox viruses. *In* Fundamental Virology. B. N. Fields and D. M. Knape, editors. Raven Press, New York. 637–655.

Ohnesorge, F. 1990. Kraftmikroskopie an biologischen Systemen. Diplomarbeit LMU/TU München, August 1990.

Ohnesorge, F. 1994. Einige Grenzanwendungen der Kraftmikroskopie. Dissertation, Ludwig Maximilian Universität München, September 1994.

Ohnesorge, F., and G. Binnig. 1993. True atomic resolution by atomic force microscopy through repulsive and attractive forces. *Science.* 260: 1451–1454.

Ohnesorge, F., W. M. Heckl, W. Haberle, H.-J. Schindler, K. Schilcher, A. Kiener, D. Pum, M. Sara, D. P. E. Smith, U. B. Sleytr, and G. Binnig. 1992. SFM studies of the s-layers from *Bacillus coagulans* E38–66, *Bacillus sphericus* CCM2177, and of an antibody binding process. *Ultramicroscopy.* 42-44:1236–1242.

Payne, L. G., and K. Kristenson. 1979. *J. Virol.* 32:614–622.

Payne, L. G., and K. Kristenson. 1982. The effect of cytochalasin D and monenin on enveloped vaccinia virus release. *Arch. Virol.* 74:11–20.

Radmacher M., M. Fritz, H. G. Hansma, and P. K. Hansma. 1994. Direct observation of enzyme activity by AFM. *Science.* 265:1577–1579.

Radmacher, M., R. W. Tillmann, M. Fritz, and H. E. Gaub. 1992. From molecules to cells: imaging soft samples with the atomic force microscope. *Science.* 257:1900.

Radmacher, M., R. W. Tillmann, and H. E. Gaub. 1993. Imaging viscoelasticity by force modulation with the atomic force microscope. *Biophys. J.* 64:735–742.

Rodriguez, J. F., E. Paez, and M. Esteban. 1986. A 14-kD envelope protein of vaccinia virus is involved in cell fusion and forms covalently linked trimers. *J. Virol.* 61:395–404.

Schabert, F., C. Henn, and A. Engel. 1995. Native e-coli OmpF porin surfaces probed with AFM. *Science.* 268:92–94.

Schaeffer, T. E., J. P. Cleveland, F. Ohnesorge, D. A. Walters, and P. K. Hansma. 1996. Studies of vibrating atomic force microscope cantilevers in liquid. *J. Appl. Physiol.* 80:3622–3627.

Schoenenberger, C.-A., and J. H. Hoh. 1994. Slow cellular dynamics in MDCK and R5 cells monitored by time-lapse AFM. *Biophys. J.* 67: 929–936.

Shroff, S. G., D. R. Saner, and R. Lal. 1995. Dynamic micromechanical properties of cultured rat atrial myocytes measured by AFM. *Am. J. Physiol.* 269:C286–C292.

Sodeik, B. 1992. Dissertation. Ruprecht-Karls-Universität Heidelberg.

Sodeik, B., G. Griffiths, M. Ericsson, B. Moss, and R. W. Doms. 1994. Assembly of vaccinia virus: effects of rifampin on the intracellular distribution of viral protein p60. *J. Virol.* 68:1103–1114.

Spudich, A., and D. Braunstein. 1995. Large secretory structures at the cell surface imaged with scanning force microscopy. *Proc. Natl. Acad. Sci. USA.* 92:6976–6980.

Stern, W., and S. Dales. 1976. Biogenesis of vaccinia virus of the envelope to virus assembly. *Virology.* 75:232–241.

Stokes, G. V. 1976. High voltage electron microscope study of the release of vaccinia virus from whole cells. *J. Virol.* 18:636–643.

Stolz, D. B., and M. D. Summers. 1972. *J. Ultrastruct. Res.* 40:581–598.

Strey, H., M. Peterson, and E. Sackmann. 1995. Measurement of erythrocyte membrane elasticity by flicker eigenmode decomposition. *Biophys. J.* 69:478–488.

Thorpe, W. P., M. Toner, R. M. Ezzell, R. G. Tompkins, et al. 1995. Dynamics of photoinduced cell plasma membrane injury. *Biophys. J.* 68:2198–2206

Tsutsui, K., F. Uno, K. Akatsuka, and S. Nii. 1983. *Arch. Virol.* 75: 213–218.

Yang, J., K. Tamm, T. W. Tillack, and Z. Shao. 1993. New approach for AFM of membrane proteins: the imaging of cholera toxin. *J. Mol. Biol.* 229:286.

Zemann, E., Engelhard, and E. Sackmann. 1990. *Eur. Biophys. J.* 18: 203–219.